

CANDELS: THE PROGENITORS OF COMPACT QUIESCENT GALAXIES AT $Z \sim 2$

GUILLERMO BARRO¹, S. M. FABER¹, PABLO G. PÉREZ-GONZÁLEZ^{2,3}, DAVID C. KOO¹, CHRISTINA C. WILLIAMS⁴, DALE D. KOCEVSKI¹, JONATHAN R. TRUMP¹, MARK MOZENA¹, ELIZABETH MCGRATH¹, ARJEN VAN DER WEL⁵, STIJN WUYTS⁶, ERIC F. BELL⁷, DARREN J. CROTON⁸, AVISHAI DEKEL⁹, M. L. N. ASHBY¹⁰, HENRY C. FERGUSON¹¹, ADRIANO FONTANA¹², MAURO GIAVALISCO⁴, NORMAN A. GROGIN¹¹, YICHENG GUO⁴, NIMISH P. HATHI¹³, PHILIP F. HOPKINS¹⁴, KUANG-HAN HUANG¹¹, ANTON M. KOEKEMOER¹¹, JEYHAN S. KARTALTEPE¹⁵, KYOUNG-SOO LEE¹⁶, JEFFREY A. NEWMAN¹⁷, LAUREN A. PORTER¹, JOEL R. PRIMACK¹, RUSSELL E. RYAN¹¹, DAVID ROSARIO⁶, RACHEL S. SOMERVILLE¹⁸

Submitted to the Astrophysical Journal Letters

ABSTRACT

We combine high-resolution *HST*/WFC3 images with multi-wavelength photometry to track the evolution of structure and activity of massive ($M_\star > 10^{10} M_\odot$) galaxies at redshifts $z = 1.4 - 3$ in two fields of the Cosmic Assembly Near-infrared Deep Extragalactic Legacy Survey (CANDELS). We detect compact, star-forming galaxies (cSFGs) whose number densities, masses, sizes, and star formation rates qualify them as likely progenitors of compact, quiescent, massive galaxies (cQGs) at $z = 1.5 - 3$. At $z \gtrsim 2$, most cSFGs have specific star-formation rates ($\text{sSFR} \sim 10^{-9} \text{yr}^{-1}$) half that of typical, massive SFGs at the same epoch, and host X-ray luminous AGNs 30 times ($\sim 30\%$) more frequently. These properties suggest that cSFGs are formed by gas-rich processes (mergers or disk-instabilities) that induce a compact starburst and feed an AGN, which, in turn, quench the star formation on dynamical timescales (few 10^8yr). The cSFGs are continuously being formed at $z = 2 - 3$ and fade to cQGs down to $z \sim 1.5$. After this epoch, cSFGs are rare, thereby truncating the formation of new cQGs. Meanwhile, down to $z = 1$, existing cQGs continue to enlarge to match local QGs in size, while less-gas-rich mergers and other secular mechanisms shepherd (larger) SFGs as later arrivals to the red sequence. In summary, we propose two evolutionary tracks of QG formation: an early ($z \gtrsim 2$), fast-formation path of rapidly-quenched cSFGs fading into cQGs that later enlarge within the quiescent phase, and a slow, late-arrival ($z \lesssim 2$) path in which larger SFGs form extended QGs without passing through a compact state.

Subject headings: galaxies: starburst — galaxies: photometry — galaxies: high-redshift

1. INTRODUCTION

Nearby galaxies come in two flavors (Kauffmann et al. 2003): red quiescent galaxies (QGs) with old stellar populations, and blue young star-forming galaxies (SFGs). This color bimodality seems to be already in place at $z \sim 2-3$ (Ilbert et al. 2010; Brammer et al. 2011), presenting also strong correlations with mass, size and morphology: SFGs are typically larger than QGs of the same mass (Williams et al. 2010; Wuyts et al. 2011b) and disk-like, whereas QGs are typically spheroids characterized by concentrated light profiles (Bell et al. 2011). Since SFGs are the progenitors of QGs, their very-different, mass-size relations restrict viable formation mechanisms.

A major surprise has been the discovery of smaller

sizes for massive QGs at higher redshifts – these compact QGs (cQGs), also colloquially known as “red nuggets”, are ~ 5 times smaller than local, equal-mass analogs (Trujillo et al. 2007; Cassata et al. 2011; Szomoru et al. 2011). In contrast, most of the massive SFGs at these redshifts are still relatively large disks (Kriek et al. 2009a). We adopt the view that galaxy mass growth is accompanied by size growth, as suggested by the mass-size relation. In this case, to form compact QGs from SFGs, three changes are required: a significant shrinkage in radius, an increase in mass concentration, and a rapid truncation of the star formation.

Proposed mechanisms to create compact spheroids from star-forming progenitors generally involve violent, dynamical processes (Naab et al. 2007), such as gas-rich mergers (Hopkins et al. 2006) or dynamical instabilities fed by cold streams (Dekel et al. 2009). Recent hydrodynamical simulations of mergers have reproduced some of the observed properties of cQGs (Wuyts et al. 2010), if high amounts of cold gas, as observed by Tacconi et al. (2010), are adopted.

If cQGs are so formed, we expect to see a co-existing population of compact SFGs and recently-quenched galaxies at $z \gtrsim 2$. Recent works demonstrate the existence of such populations (Cava et al. 2010; Wuyts et al. 2011b; Whitaker et al. 2012), but a direct evolutionary link has not yet been clearly established.

This letter shows a quantitative connection between cSFGs and QGs at high- z . We combine the deepest

¹ University of California, Santa Cruz

² Universidad Complutense de Madrid

³ Steward Observatory, University of Arizona

⁴ University of Massachusetts

⁵ Max-Planck-Institut für Astronomie

⁶ Max-Planck-Institut für extraterrestrische Physik

⁷ Department of Astronomy, University of Michigan

⁸ Swinburne University of Technology

⁹ The Hebrew University

¹⁰ Harvard-Smithsonian Center for Astrophysics

¹¹ Space Telescope Science Institute

¹² INAF Osservatorio Astronomico di Roma

¹³ Observatories of the Carnegie Institution of Washington

¹⁴ University of California Berkeley

¹⁵ National Optical Astronomy Observatory

¹⁶ Purdue University

¹⁷ University of Pittsburgh

¹⁸ Rutgers University

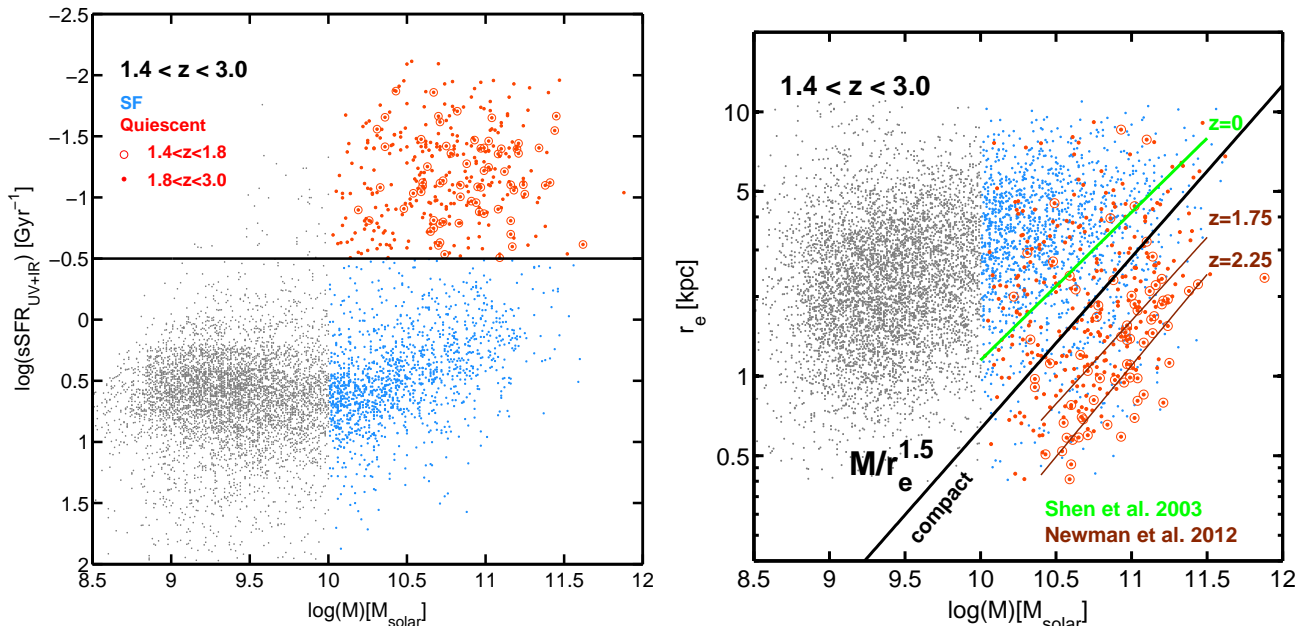


FIG. 1.— *Left panel:* Specific SFR as a function of the stellar mass for galaxies at $1.4 < z < 3.0$. The solid black line defines our threshold, $\log(\text{sSFR}) = -0.5$, to select QGs (red in both panels) and SFGs (blue) above $M_{\star} > 10^{10} M_{\odot}$. Grey dots show galaxies with stellar masses below the mass selection limit. *Right panel:* Stellar mass-size relation at $1.4 < z < 3.0$. The solid black line defines our selection criterion for compact galaxies, $M/r_e^{1.5} = 10.3 M_{\odot} \text{kpc}^{-1.5}$. The green line shows the local mass-size relation for elliptical galaxies (Shen et al. 2003). The thin brown lines are the mass-size relations for QGs found at $z = 1.75$ and $z = 2.25$ by Newman et al. (2012).

photometric data from the optical to the far IR from the Great Observatories Origins Deep Survey (GOODS; Giavalisco et al. 2004), the UKIDSS Ultra Deep Survey (UDS), the Cosmic Assembly Near-infrared Deep Extragalactic Legacy Survey (CANDELS; Grogin et al. 2011; Koekemoer et al. 2011), FIDEL¹⁹, and SpUDS²⁰ to estimate stellar masses, SFRs, and sizes for massive, high- z galaxies. By analyzing the global evolution in the space defined by these parameters, we suggest two paths (fast and slow) for QG formation from $z \sim 3$ to $z \sim 1$.

We adopt a flat cosmology with $\Omega_M = 0.3$, $\Omega_{\Lambda} = 0.7$ and $H_0 = 70 \text{ km s}^{-1} \text{ Mpc}^{-1}$.

2. DATA DESCRIPTION AND SAMPLE SELECTION

This letter is based on a sample of massive galaxies built from the *HST*/WFC3 F160W (*H*-band) selected catalog ($H_{5\sigma}(\text{AB}) = 27 \text{ mag}$) for the GOODS-S and UDS fields of CANDELS. Consistent, multi-wavelength photometry (*U*-band to $8 \mu\text{m}$) was measured using TFIT (Laidler et al. 2006), implemented as described by Guo et al. (2011) and Galametz et al. (2012, in prep.). Photometric redshifts were computed using EAZY (Brammer et al. 2008) and yielded errors of $\Delta z/(1+z) = 3\%$ and 6% at $z > 1.5$ in GOODS-S and UDS, respectively. This dataset is partially described in Wuyts et al. (2011b); for full details, see Dahlen et al. (2012, in prep.). Stellar masses were derived using FAST (Kriek et al. 2009b) and based on a grid of Bruzual & Charlot (2003) models that assume a Chabrier (2003) IMF, solar metallicity, exponentially declining star formation histories, and the Calzetti et al. (2000) dust extinction law.

SFRs were computed by combining IR and rest-frame UV (uncorrected for extinction) luminosities (Kennicutt

1998 and Bell et al. 2005) and adopting a Chabrier (2003) IMF: $\text{SFR}_{\text{UV+IR}} = 1.09 \times 10^{-10} (L_{\text{IR}} + 3.3 L_{2800})$. Total IR luminosities ($L_{\text{IR}} \equiv L[8-1000 \mu\text{m}]$) were derived from Chary & Elbaz (2001) templates fitting MIPS $24 \mu\text{m}$ fluxes, applying a *Herschel*-based re-calibration (Elbaz et al. 2011). For galaxies undetected by MIPS below a 2σ level ($20 \mu\text{Jy}$) and for galaxies detected in the X-rays, SFRs come from rest-frame UV luminosities that are corrected for extinction as derived from SED fits (Wuyts et al. 2011a). $L_X \equiv L_{2-8 \text{ keV}}$ were computed for the sources in the *Chandra* 4Ms image in GOODS-S (Xue et al. 2011) and the XMM 50–100ks survey in UDS (Ueda et al. 2008). Due to the shallower detection limits in the IR and X-ray surveys of UDS, the detection fractions are computed only on GOODS-S data.

Circularized, effective (half-light) radii, $r_e \equiv a \sqrt{(b/a)}$, and Sèrsic indices were measured from *HST*/WFC3 *H* images using GALFIT (Peng et al. 2002) and PSFs created and processed to replicate the conditions of the observed data (van der Wel et al. 2011, and 2012 in prep.).

We selected a sample of galaxies at $1.4 < z < 3.0$ with $M_{\star} > 10^{10} M_{\odot}$, above which our sample is $>90\%$ complete up to the highest redshifts (Wuyts et al. 2011b; Newman et al. 2012). Compact galaxies were based on *H*-band sizes; quiescent galaxies (QGs) and star-forming galaxies (SFGs) were separated by a specific SFR (sSFR) of $10^{-0.5} \text{ Gyr}^{-1}$ (see Figure 1). Although somewhat arbitrary, the value does not strongly affect the results, since the sSFR bimodality is clearly detected up to $z = 3$.

Figure 1 also shows a mass-size diagram for our sample. In agreement with recent results, we find that SFGs and QGs follow significantly different mass-size relations (Williams et al. 2010; Wuyts et al. 2011b). With this in mind, we select compact galaxies as those following the observed trend in the mass-size relation for QGs at $z > 1.5$. The threshold is defined as $M/r_e^{\alpha} = 10.3 M_{\odot} \text{kpc}^{-\alpha}$,

¹⁹ <http://irsa.ipac.caltech.edu/data/SPITZER/FIDEL/>

²⁰ <http://irsa.ipac.caltech.edu/data/SPITZER/SpUDS/>

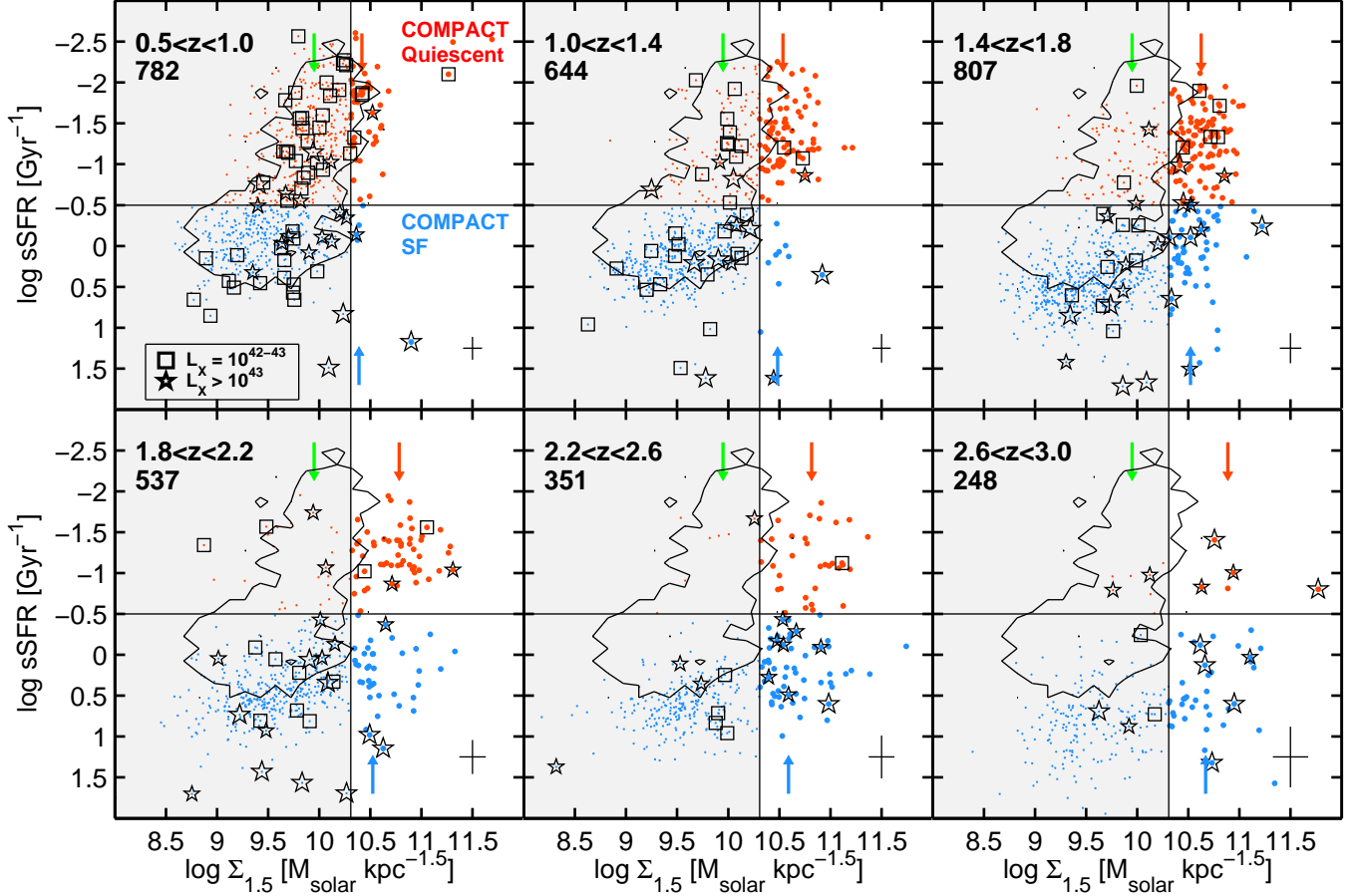


FIG. 2.— Evolution of the sSFR vs. $\Sigma_{1.5} \equiv M/r_e^{1.5}$ correlation at $0.5 < z < 3.0$ for galaxies above $M_* > 10^{10} M_\odot$. The redshift bins are chosen to probe similar comoving volumes. The solid lines and colored dots depict the selection thresholds for SFGs (blue) and QGs (red) and compact (white region) and non-compact (shaded region), as defined in Figure 1. The open markers depict sources detected in the X-rays at different luminosities: squares have $10^{42} < L_X < 10^{43}$ erg/s; small (large) stars have $L_X > 10^{43}$ (10^{44} ; i.e. QSO) erg/s. Blue and red arrows indicate the median $\Sigma_{1.5}$ of cSFGs and cQGs, respectively. Green arrows approximate the local mass-size relation (Shen et al. 2003). The black contour shows the sSFR- $\Sigma_{1.5}$ distribution for 90% of the galaxies at $0.5 < z < 1.0$. The lower-right error bars for $\Sigma_{1.5}$ and the SFR include uncertainties in: half-light radii, stellar masses, rest-frame luminosities (derived by perturbing photometric redshifts within the 1σ errors), and the average *rms* of the comparison between UV-corrected and (UV+IR)-based SFR estimates.

with $\alpha = 1.5$. The slope is roughly consistent with those given by Newman et al. (2012) for QGs at similar redshifts ($\alpha^{-1} = 0.59-0.69$). The zero-point is chosen to include the majority of QGs with minimum contamination from SFGs. For $\alpha = 1.5$, M/r_e^α (hereafter, $\Sigma_{1.5}$) lies between the surface density, $\Sigma = M/r_e^2$, and M/r_e , both of which follow strong correlations with color and SFR up to high redshifts (e.g., Franx et al. 2008).

Figure 2 shows the evolution of sSFRs vs. $\Sigma_{1.5}$ for massive galaxies from $z = 3.0$ down to $z = 0.5$. In this diagram, our size-mass-SFR selection is completely orthogonal. Although our analysis focuses on $z > 1.4$, two panels at lower redshifts are shown to illustrate the extrapolated evolutionary trends. We find that the number of QGs (above the line) increases rapidly since $z = 3$, starting from very small number densities, $n \sim 10^{-5} \text{ Mpc}^{-3}$, at $z \sim 2.8$. Among these, the number of compact QGs (cQG; $\Sigma_{1.5} > 10.3$) builds up first, and only at $z < 1.8$ we do start finding a sizable number of extended QGs. This suggests that the bulk of these galaxies are assembled at late times by both continuous migration (quenching) of non-compact SFGs (bottom-left region) and size growth of cQGs. As a result of this growth, the population of

cQGs disappears by $z \sim 1$. Simultaneously, we identify a population of compact SFGs (cSFGs) whose number density decreases steadily with time since $z = 3.0$, being almost completely absent at $z < 1.4$. The number of cSFGs makes up less than 20% of all massive SFGs, but they present similar number densities as cQGs down to $z \sim 2$, suggesting an evolutionary link between the two populations.

3. CO-EVOLUTION OF COMPACT SFGS AND QGS

An evolutionary sequence where cSFGs are the progenitors of cQGs at lower redshifts is supported by the fact that cSFGs first appear before cQGs at high redshift ($z = 2.6 - 3.0$) and then disappear before them at low redshift ($z = 1.0 - 1.4$), implying that evolution is from blue through red rather than vice versa. Therefore, if we assume that cSFGs would see their star formation quenched and fade at roughly constant $\Sigma_{1.5}$, these could rapidly populate the compact quiescent region in time scales of $\sim 500 \text{ Myr}$ (approx. one of our redshift intervals).

A more detailed analysis of the sizes of cSFGs and cQGs shows that, indeed, both populations have median effective radii slightly smaller than 1 kpc (similar to the

findings in van der Wel et al. 2011; Szomoru et al. 2011). The median $\Sigma_{1.5}$ of cQGs (red arrows in Figure 2) decrease by 0.25 dex (i.e., increase their radii by a factor of ~ 2) from $z=3.0$ to $z=1.4$, in agreement with previous results on the size evolution of QGs (Cassata et al. 2011), whereas cSFGs present smaller values of $\Sigma_{1.5}$ (blue arrows) by ~ 0.2 dex, and a weaker evolution with time. However, cSFGs migrating to the red sequence are expected to slowly increase their masses with time, thus moving to higher values of $\Sigma_{1.5}$ at lower redshifts. Given their median sSFR, the typical mass-doubling times for cSFGs range from 0.6 to 1 Gyr. This is enough to account for the observed difference in $\Sigma_{1.5}$ between cSFGs and cQGs, provided that the newly formed stars do not significantly increase the galaxy radii.

Both cQGs and cSFGs present similar surface brightness profiles, which are best represented by large Sérsic indices. The median values range from $n = 3 - 4$ for cQGs to $n = 2.5 - 3.5$ for cSFGs. This means that both populations are preferentially spheroid-like, in contrast with non-compact, disk-like SFGs ($n \sim 1$). The median axis ratios of cSFGs, $b/a \sim 0.65$, are also consistent with spheroidal morphologies. However, cQGs present slightly smaller axis-ratios, $b/a \sim 0.54$, suggesting that some of these are small flattened disks (van der Wel et al. 2011). This feature might be explained if cQGs developed an extended component surrounding the compact core, perhaps via minor mergers (Naab & Ostriker 2009) or regrowth of a remnant disk that survived the major merger (Governato et al. 2009; Hopkins et al. 2009). These mechanisms will continue to grow these galaxies in size, eventually depopulating the compact region.

Turning back to the possibility of cSFGs fading into cQGs, we find that indeed cSFGs present suppressed sSFRs compared to the bulk of SFGs. Although at $z > 2$ the majority ($\sim 60-80\%$) of cSFGs are detected at $24\mu\text{m}$, yielding $\text{SFR} = 100-200 \text{ M}_\odot/\text{yr}^{-1}$, their median sSFRs are typically ~ 0.3 dex lower than those for non-compact SFGs at the same redshift. This suggests that the star formation in the compact evolutionary stage already has started to quench.

Simultaneously, we find an increasing fraction of cSFGs hosting X-ray detected Active Galactic Nuclei (AGN) at $z > 2$ (open markers in Figure 2). This result also supports the quenching scenario, since AGN seems to be connected with quenching of the star formation on time scales of a few hundred Myrs (Hopkins et al. 2006). In particular, a high luminosity quasar phase ($L_X > 10^{44} \text{ erg s}^{-1}$), associated with high black-hole accretion rates, would be particularly efficient at removing the available gas, thus stopping the star formation. Using data from the deepest X-ray survey in GOODS-S, we find that cSFGs host X-ray luminous AGNs 30x ($\sim 30\%$) more frequently than non-compact ($< 1\%$) (but massive) SFGs at $z \gtrsim 2.2$. This implies that, at these epochs, the majority of luminous ($L_X > 10^{43} \text{ erg/s}$) AGN are found preferentially in compact hosts, as opposed to lower redshifts, where AGN are more frequent in non-compact galaxies (Kocevski et al. 2012). Interestingly, (the few) cQGs at $z \sim 2.8$ also show a high fraction of X-ray detections ($> 70\%$), strengthening the idea that AGNs might play an important role on the quenching of star formation.

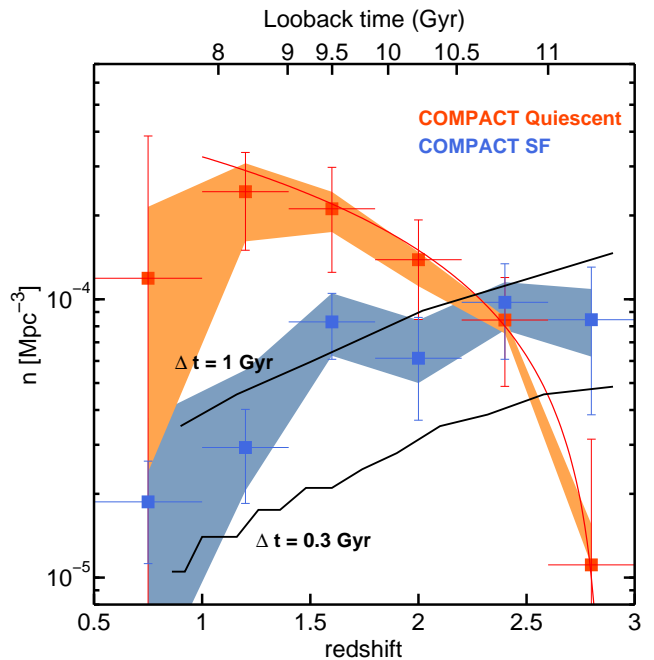


FIG. 3.— Number density evolution of massive, $M_* > 10^{10} \text{ M}_\odot$, cQGs (red) and cSFGs (blue) versus redshift. The solid red line is the best fit to the number density of cQGs. Solid black lines depict the evolution of the number of cSFGs required to match the observed increasing density of cQGs, assuming that the former have lifetimes of $\Delta t_{\text{burst}} = 0.3 - 1$ Gyr. The error bars were computed by bootstrapping the sSFR and $\Sigma_{1.5}$ uncertainties along with terms for small number statistics and field-to-field differences. The shaded regions encompass the observed number densities when the selection thresholds in sSFR and $\Sigma_{1.5}$ are modified by ± 0.2 dex.

Note that, although point source contamination from a luminous AGN could bias the structural parameters towards compact morphologies (Pierce et al. 2010), X-ray detected galaxies do not deviate from the general trend followed by non-X-ray detected cSFGs in Figure 2, with the exception of a few extreme outliers. These AGNs and also those with strong SED contamination were excluded from our sample prior to the analysis described above.

4. NUMBER DENSITY OF COMPACT GALAXIES

Figure 3 shows the number density evolution of massive cQGs and cSFGs. The best fit (red line) to the increasing number density of QGs can be parametrized as $n = a + b(1+z)$, with $a = 1.75 \times 10^{-4}$ and $b = -6.75 \times 10^{-4}$. Assuming that all cQGs at a given redshift z' come from cSFGs, we can estimate how many of the latter we should observe at $z > z'$. To do so, we propose a simple evolutionary model that assigns to all SFGs an arbitrary lifetime for their current burst of star formation, Δt_{burst} , after which they will become quiescent. The number of cQGs at a given time would be:

$$n_{\text{QG}}(t + \Delta t_{\text{burst}}) = n_{\text{QG}}(t) + n_{\text{SFG}}(t) \quad (1)$$

We explore Δt_{burst} values from 0.3 Gyr to 1.0 Gyr, similar to the typical e-folding times expected for SFGs at these redshifts (Wuyts et al. 2011a). The observed number density of cSFGs is broadly consistent with the model prediction for a median value of $\Delta t_{\text{burst}} \sim 800$ Myr.

This simple model assumes, that at every step, Δt_{burst} , enough cSFGs are being formed by some mechanism(s), restoring the ones that turned into cQGs. Plausible

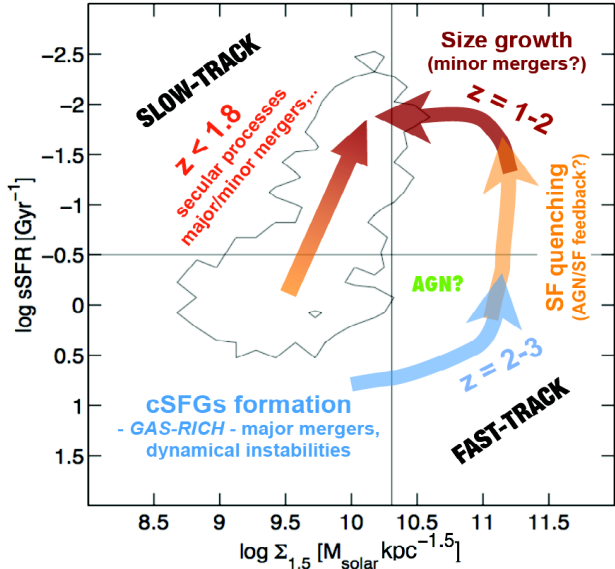


FIG. 4.— Schematic view of a two path (fast/slow track) formation scenario for QGs. On the fast track, a small fraction of the massive SFGs at $z = 2 - 3$ evolve (e.g., through gas-rich dissipational processes) to a compact star-bursting remnant. Then, the star formation is quenched in ~ 800 Myr (perhaps by AGN and/or supernovae feedback), and galaxies fade into cQGs. Once in the red sequence, cQGs grow envelopes, over longer time scales, de-populating the compact region by $z \sim 1$. Simultaneously, at $z \lesssim 2$, other (slower) mechanisms have already started to populate the red-sequence with normal-sized, non-compact QGs (formed by, e.g., secular processes, halo quenching, or gas-poor mergers)

mechanisms to reduce the size of massive (larger) SFGs are gas-rich dissipational processes, such as mergers or dynamical instabilities. These can produce compact, star-bursting remnants that would likely quench in a short period of time (Hopkins et al. 2006; Dekel et al. 2009). Without relying on mergers being the main or sole driver of this transformation, we can make a quantitative estimate of the number of cSFGs assembled by this mechanism by using typical numbers for major mergers at these redshifts. Considering pair fractions of roughly 10% (Williams et al. 2011), merger time scales of 1 Gyr (Lotz et al. 2011) and a density of massive galaxies of $\lesssim 10^{-3} \text{ Mpc}^{-3}$ (Pérez-González et al. 2008), we obtain an assembly rate for new cSFGs via mergers of $\Delta n_{\text{cSFG}} \sim 10^{-4} \text{ Gyr}^{-1}$, which is roughly consistent with the observed densities for the predicted Δt_{burst} .

In this model, the significant decrement on the number cSFGs by $z < 1.4$ implies that the formation mechanism(s) become quickly inefficient at lower redshifts, thereby truncating the formation of new cSFGs and thus cQGs. This gradual decline of the efficiency of the dissipational processes may follow the decline in the amount of available gas in dark matter haloes (e.g., Croton 2009). Detailed comparisons to cosmological models will allow tests of this hypothesis and provide a more rigorous modeling of the number density evolution (Porter et al., in prep). Also, a follow up survey of cSFGs at $z \gtrsim 3$ will place better constraints on the formation scenario for these galaxies (C. Williams et al., in prep).

5. SUMMARY AND DISCUSSION

Using the deepest data spanning from the X-ray-to-MIR, along with high resolution imaging from CAN-

DELS in GOODS-S and UDS, we analyze stellar masses, SFRs and sizes of a sample of massive ($M_* > 10^{10} M_\odot$) galaxies at $z = 1.4 - 3.0$ to identify a population of cSFGs with similar structural properties as cQGs at $z \gtrsim 2$. The cSFG population is already in place at $z \sim 3$, but it completely disappears by $z < 1.4$. A corresponding increase in the number of cQGs during the same time period suggests an evolutionary link between them.

A simple duty-cycle argument, involving quenching of the star formation activity on time scales of $\Delta t = 0.3 - 1$ Gyr, is able to broadly reproduce the evolution of the density of new QGs formed since $z = 3$ in terms of fading cSFGs. Under this assumption, we also need to invoke a replenishment mechanism to form new cSFG via gas-rich dissipational processes (major mergers or dynamical instabilities), that then become quickly inefficient at $z \lesssim 1.5$, as the amount of available gas in the halo decreases with time (e.g., Croton 2009).

During the transformation processes, the compact phase is probably associated with: enhanced (probably nuclear and dusty) star formation, the presence of an AGN, and sometimes a short-lived quasar, followed by a decline of the star formation in ~ 1 Gyr (Hopkins et al. 2006). All these phenomena fit with the observed properties of cSFGs presented in this letter. cSFGs present no visible traces of mergers, but they do show lower sSFRs than the bulk of massive SFGs, presumably being at different stages of the starburst to passive evolution. Simultaneously, $\sim 30\%$ of them host luminous ($L_X > 10^{43} \text{ erg s}^{-1}$) X-ray detected AGNs at $z > 2$, suggesting that these might be playing a role in the quenching of star formation.

Our observations connect two recent results at $z \sim 2$: a population of compact ($n \gtrsim 2$) galaxies with enhanced star formation activity (Wuyts et al. 2011b) and an increasing fraction of small, post-starburst galaxies recently arrived on the red sequence (Whitaker et al. 2012). The emerging picture suggests that the formation of QGs follows two evolutionary tracks, each one dominating at different epochs (as illustrated in Figure 4). At $z \gtrsim 2$ the formation of QGs proceeds on a fast track (right-region): from $z = 3.0 - 2.0$, the number of cQGs builds up rapidly upon quenching of cSFGs at roughly constant $\Sigma_{1.5}$. Merely 2 Gyrs later ($z \sim 1$), cQGs almost completely disappear due to: 1) size growth as a result of minor mergers satellite accretion (Naab & Ostriker 2009; Newman et al. 2012) or the re-growth of a remnant disk (Hopkins et al. 2009) which causes them to leave the compact region; 2) a decrement in the efficiency of the formation mechanisms for new cSFGs, and therefore new cQGs. By $z \lesssim 2$, other (probably slower) mechanisms start to populate the red sequence with larger, non-compact, QGs without passing through a compact state. This slow track (left region) is likely associated with the fading of normal disk galaxies to become S0s, due to halo quenching (Birnboim & Dekel 2003) or morphological quenching (Martig et al. 2009). Alternatively, some of these QGs could also be the result late and less-gas-rich mergers.

ACKNOWLEDGMENTS

Support for Program number HST-GO-12060 was provided by NASA through a grant from the Space Telescope Science Institute, which is operated by the Asso-

ciation of Universities for Research in Astronomy, In-

corporated, under NASA contract NAS5-26555. PGP-G acknowledges support from grant AYA2009-07723-E.

REFERENCES

- Bell, E. F., Papovich, C., Wolf, C., et al. 2005, *ApJ*, 625, 23
- Bell, E. F., van der Wel, A., Papovich, C., et al. 2011, *ArXiv e-prints*
- Birnboim, Y. & Dekel, A. 2003, *MNRAS*, 345, 349
- Brammer, G. B., van Dokkum, P. G., & Coppi, P. 2008, *ApJ*, 686, 1503
- Brammer, G. B., Whitaker, K. E., van Dokkum, P. G., et al. 2011, *ApJ*, 739, 24
- Bruzual, G. & Charlot, S. 2003, *MNRAS*, 344, 1000
- Calzetti, D., Armus, L., Bohlin, R. C., et al. 2000, *ApJ*, 533, 682
- Cassata, P., Giavalisco, M., Guo, Y., et al. 2011, *ApJ*, 743, 96
- Cava, A., Rodighiero, G., Pérez-Fournon, I., et al. 2010, *MNRAS*, 409, L19
- Chabrier, G. 2003, *PASP*, 115, 763
- Chary, R. & Elbaz, D. 2001, *ApJ*, 556, 562
- Croton, D. J. 2009, *MNRAS*, 394, 1109
- Dekel, A., Sari, R., & Ceverino, D. 2009, *ApJ*, 703, 785
- Elbaz, D., Dickinson, M., Hwang, H. S., et al. 2011, *A&A*, 533, A119
- Franx, M., van Dokkum, P. G., Schreiber, N. M. F., et al. 2008, *ApJ*, 688, 770
- Giavalisco, M., Ferguson, H. C., Koekemoer, A. M., et al. 2004, *ApJ*, 600, L93
- Governato, F., Brook, C. B., Brooks, A. M., et al. 2009, *MNRAS*, 398, 312
- Grogin, N. A., Kocevski, D. D., Faber, S. M., et al. 2011, *ApJS*, 197, 35
- Guo, Y., Giavalisco, M., Cassata, P., et al. 2011, *ApJ*, 735, 18
- Hopkins, P. F., Hernquist, L., Cox, T. J., et al. 2006, *ApJS*, 163, 1
- Hopkins, P. F., Hernquist, L., Cox, T. J., Keres, D., & Wuyts, S. 2009, *ApJ*, 691, 1424
- Ilbert, O., Salvato, M., Le Floc'h, E., et al. 2010, *ApJ*, 709, 644
- Kauffmann, G., Heckman, T. M., White, S. D. M., et al. 2003, *MNRAS*, 341, 54
- Kennicutt, Jr., R. C. 1998, *ARA&A*, 36, 189
- Kocevski, D. D., Faber, S. M., Mozena, M., et al. 2012, *ApJ*, 744, 148
- Koekemoer, A. M., Faber, S. M., Ferguson, H. C., et al. 2011, *ApJS*, 197, 36
- Kriek, M., van Dokkum, P. G., Franx, M., Illingworth, G. D., & Magee, D. K. 2009a, *ApJ*, 705, L71
- Kriek, M., van Dokkum, P. G., Labbé, I., et al. 2009b, *ApJ*, 700, 221
- Laidler, V. G., Grogin, N., Clubb, K., et al. 2006, in *Astronomical Society of the Pacific Conference Series*, Vol. 351, *Astronomical Data Analysis Software and Systems XV*, ed. C. Gabriel, C. Arviset, D. Ponz, & S. Enrique, 228
- Lotz, J. M., Jonsson, P., Cox, T. J., et al. 2011, *ApJ*, 742, 103
- Martig, M., Bournaud, F., Teyssier, R., & Dekel, A. 2009, *ApJ*, 707, 250
- Naab, T., Johansson, P. H., Ostriker, J. P., & Efstathiou, G. 2007, *ApJ*, 658, 710
- Naab, T. & Ostriker, J. P. 2009, *ApJ*, 690, 1452
- Newman, A. B., Ellis, R. S., Bundy, K., & Treu, T. 2012, *ApJ*, 746, 162
- Peng, C. Y., Ho, L. C., Impey, C. D., & Rix, H.-W. 2002, *AJ*, 124, 266
- Pérez-González, P. G., Rieke, G. H., Villar, V., et al. 2008, *ApJ*, 675, 234
- Pierce, C. M., Lotz, J. M., Primack, J. R., et al. 2010, *MNRAS*, 405, 718
- Shen, S., Mo, H. J., White, S. D. M., et al. 2003, *MNRAS*, 343, 978
- Szomoru, D., Franx, M., Bouwens, R. J., et al. 2011, *ApJ*, 735, L22
- Tacconi, L. J., Genzel, R., Neri, R., et al. 2010, *Nature*, 463, 781
- Trujillo, I., Conselice, C. J., Bundy, K., et al. 2007, *MNRAS*, 382, 109
- Ueda, Y., Watson, M. G., Stewart, I. M., et al. 2008, *ApJS*, 179, 124
- van der Wel, A., Rix, H.-W., Wuyts, S., et al. 2011, *ApJ*, 730, 38
- Whitaker, K. E., Kriek, M., van Dokkum, P. G., et al. 2012, *ApJ*, 745, 179
- Williams, R. J., Quadri, R. F., & Franx, M. 2011, *ApJ*, 738, L25
- Williams, R. J., Quadri, R. F., Franx, M., et al. 2010, *ApJ*, 713, 738
- Wuyts, S., Cox, T. J., Hayward, C. C., et al. 2010, *ApJ*, 722, 1666
- Wuyts, S., Förster Schreiber, N. M., Lutz, D., et al. 2011a, *ApJ*, 738, 106
- Wuyts, S., Förster Schreiber, N. M., van der Wel, A., et al. 2011b, *ApJ*, 742, 96
- Xue, Y. Q., Luo, B., Brandt, W. N., et al. 2011, *ApJS*, 195, 10